

Temperature behavior of the magnon modes of the square lattice antiferromagnet

A. Sherman

Institute of Physics, University of Tartu, Riia 142, 51014 Tartu, Estonia

M. Schreiber

Institut für Physik, Technische Universität, D-09107 Chemnitz, Federal Republic of Germany

(December 4, 2017)

Abstract

A spin-wave theory of short-range order in the square lattice Heisenberg antiferromagnet is formulated. With growing temperature from $T = 0$ a gapless mode is shown to arise simultaneously with opening a gap in the conventional spin-wave mode. The spectral intensity is redistributed from the latter mode to the former. For low temperatures the theory reproduces results of the modified spin-wave theory by M. Takahashi, J. E. Hirsch *et al.* and without fitting parameters gives values of observables in good agreement with Monte Carlo results in the temperature range $0 \leq T \lesssim 0.8J$ where J is the exchange constant.

Properties of the spin- $\frac{1}{2}$ quantum Heisenberg antiferromagnet on a square lattice attract much attention in connection with the investigation of cuprate-perovskite high-temperature superconductors. In accord with the existing theories¹⁻⁵ the spectrum of this antiferromagnet contains the doubly degenerate (in the magnetic Brillouin zone) magnon mode which is gapless at zero temperature. For $T > 0$ in this mode a gap opens near the center of the zone. The appearance of this gap is connected with the short-range antiferromagnetic ordering which is established in two-dimensional antiferromagnets at nonzero temperature.⁶

Of special note are the spin-wave theory of Refs. 3,4 where without fitting parameters values of many observables were calculated in good agreement with the exact diagonalization and Monte Carlo calculations in the temperature range $0 \leq T \lesssim 0.6J$. Results of these works can be obtained with the mean-field decoupling of terms of the Hamiltonian which are quartic in the magnon operators or, equivalently, by decoupling of many-particle Green's functions in the equations of motion for the one-particle Green's functions.⁷ In the theory of Refs. 3,4 the gap in the finite-temperature magnon spectrum appears with imposing the constraint of zero staggered magnetization to retain the sublattice symmetry in short-range order and to ensure zero site magnetization in the absence of magnetic field. Notice that this spin-wave approximation is not rotationally invariant.

In the present paper we try to obtain a better approximation for the magnon Green's functions by transferring the decoupling to higher order equations of motion. This allows us to expand the temperature range where the theory conforms with Monte Carlo data up to $T \approx 0.8J$. Besides, in our theory, as soon as the temperature exceeds zero an additional gapless mode arises simultaneously with opening a gap in the conventional magnon mode. For large crystals and low temperatures the spectral intensity of the gapless mode is weak and our theory reproduces results of Refs. 3,4. With growing temperature the spectral intensity is redistributed from the conventional to the gapless mode.

We consider the antiferromagnetic Heisenberg model on a plane square lattice with the Hamiltonian

$$H = J \sum_{\mathbf{l}\mathbf{a}} \mathbf{S}_{\mathbf{l}} \mathbf{S}_{\mathbf{l}+\mathbf{a}}. \quad (1)$$

Here $\mathbf{S}_{\mathbf{l}}$ is the spin- $\frac{1}{2}$ operator, \mathbf{l} runs over sites of one of two sublattices, and \mathbf{a} are vectors of the four nearest neighbors of site zero. In the following discussion the exchange constant J is taken as the unit of energy.

The Dyson-Maleev transformation⁸ is used to represent the spin operators by boson operators $a_{\mathbf{l}}$ and $b_{\mathbf{m}}$ on the two sublattices A and B

$$\begin{aligned} S_{\mathbf{l}}^- &= a_{\mathbf{l}}^\dagger, & S_{\mathbf{l}}^+ &= (1 - a_{\mathbf{l}}^\dagger a_{\mathbf{l}}) a_{\mathbf{l}}, & S_{\mathbf{l}}^z &= \frac{1}{2} - a_{\mathbf{l}}^\dagger a_{\mathbf{l}}, \\ \mathbf{l} &\in A, & & & & \\ & & & & & \\ S_{\mathbf{m}}^- &= -b_{\mathbf{m}}, & S_{\mathbf{m}}^+ &= -b_{\mathbf{m}}^\dagger (1 - b_{\mathbf{m}}^\dagger b_{\mathbf{m}}), & & \\ & & & & & \\ S_{\mathbf{m}}^z &= -\frac{1}{2} + b_{\mathbf{m}}^\dagger b_{\mathbf{m}}, & \mathbf{m} &\in B. & & \end{aligned} \quad (2)$$

In the new notations Hamiltonian (1) acquires the form

$$\begin{aligned}
H = & -\frac{N}{2} + 2 \sum_{\mathbf{l}} a_{\mathbf{l}}^{\dagger} a_{\mathbf{l}} + 2 \sum_{\mathbf{m}} b_{\mathbf{m}}^{\dagger} b_{\mathbf{m}} \\
& + \sum_{\mathbf{l}\mathbf{a}} \left(\frac{1}{2} a_{\mathbf{l}}^{\dagger} a_{\mathbf{l}} a_{\mathbf{l}+\mathbf{a}} + \frac{1}{2} a_{\mathbf{l}}^{\dagger} b_{\mathbf{l}+\mathbf{a}}^{\dagger} b_{\mathbf{l}+\mathbf{a}}^{\dagger} b_{\mathbf{l}+\mathbf{a}} \right. \\
& \quad \left. - a_{\mathbf{l}}^{\dagger} a_{\mathbf{l}} b_{\mathbf{l}+\mathbf{a}}^{\dagger} b_{\mathbf{l}+\mathbf{a}} - \frac{1}{2} a_{\mathbf{l}}^{\dagger} b_{\mathbf{l}+\mathbf{a}}^{\dagger} - \frac{1}{2} a_{\mathbf{l}} b_{\mathbf{l}+\mathbf{a}} \right), \tag{3}
\end{aligned}$$

where N is the total number of sites.

To investigate the spectrum of elementary excitations we shall calculate the following Green's functions:

$$D_1(\mathbf{q}t) = -i\theta(t) \langle [a_{\mathbf{q}}^{\dagger}(t), a_{\mathbf{q}}] \rangle, \tag{4}$$

$$D_2(\mathbf{q}t) = -i\theta(t) \langle [b_{-\mathbf{q}}(t), a_{\mathbf{q}}] \rangle,$$

where $a_{\mathbf{q}}^{\dagger} = (2/N)^{1/2} \sum_{\mathbf{l}} \exp(i\mathbf{q}\mathbf{l}) a_{\mathbf{l}}^{\dagger}$, $b_{\mathbf{q}} = (2/N)^{1/2} \sum_{\mathbf{m}} \exp(-i\mathbf{q}\mathbf{m}) b_{\mathbf{m}}$ with the wave vector \mathbf{q} in the magnetic Brillouin zone, $a_{\mathbf{q}}^{\dagger}(t) = \exp(iHt) a_{\mathbf{q}}^{\dagger} \exp(-iHt)$, and angular brackets denote thermodynamic averaging. Equations of motion for these Green's functions read

$$i \frac{d}{dt} D_1(\mathbf{q}t) = -\delta(t) - 2D_1(\mathbf{q}t) + 2\gamma_{\mathbf{q}} D_2(\mathbf{q}t) + D_3(\mathbf{q}t), \tag{5}$$

$$i \frac{d}{dt} D_2(\mathbf{q}t) = 2D_2(\mathbf{q}t) - 2\gamma_{\mathbf{q}} D_1(\mathbf{q}t) + D_4(\mathbf{q}t),$$

where $\gamma_{\mathbf{q}} = \frac{1}{4} \sum_{\mathbf{a}} \exp(i\mathbf{q}\mathbf{a})$ and

$$\begin{aligned}
D_3(\mathbf{q}t) &= -i\theta(t) \sqrt{\frac{2}{N}} \sum_{\mathbf{l}\mathbf{a}} e^{i\mathbf{q}\mathbf{l}} \langle [(a_{\mathbf{l}}^{\dagger}(t) b_{\mathbf{l}+\mathbf{a}}^{\dagger}(t) b_{\mathbf{l}+\mathbf{a}}(t) - a_{\mathbf{l}}^{\dagger}(t) a_{\mathbf{l}}(t) b_{\mathbf{l}+\mathbf{a}}(t)), a_{\mathbf{q}}] \rangle, \\
D_4(\mathbf{q}t) &= -i\theta(t) \sqrt{\frac{2}{N}} \sum_{\mathbf{m}\mathbf{a}} e^{i\mathbf{q}\mathbf{m}} \langle [(a_{\mathbf{m}+\mathbf{a}}^{\dagger}(t) b_{\mathbf{m}}^{\dagger}(t) b_{\mathbf{m}}(t) - a_{\mathbf{m}+\mathbf{a}}^{\dagger}(t) a_{\mathbf{m}+\mathbf{a}}(t) b_{\mathbf{m}}(t)), a_{\mathbf{q}}] \rangle.
\end{aligned}$$

The decoupling of the many-particle Green's functions D_3 and D_4 can be carried out at this stage. If, like in Ref. 4, an additional constraint of zero staggered magnetization

$$\begin{aligned}
\sum_{\mathbf{l}} S_{\mathbf{l}}^z - \sum_{\mathbf{m}} S_{\mathbf{m}}^z = 0 & \implies \\
\sum_{\mathbf{l}} a_{\mathbf{l}}^{\dagger} a_{\mathbf{l}} + \sum_{\mathbf{m}} b_{\mathbf{m}}^{\dagger} b_{\mathbf{m}} &= \frac{N}{2} \tag{6}
\end{aligned}$$

is imposed by incorporating it with a Lagrange multiplier in Hamiltonian (3) and if the correlations $C_1 = \langle a_{\mathbf{l}} b_{\mathbf{l}+\mathbf{a}} \rangle = \langle a_{\mathbf{l}}^{\dagger} b_{\mathbf{l}+\mathbf{a}}^{\dagger} \rangle$ and $\langle a_{\mathbf{l}}^{\dagger} a_{\mathbf{l}} \rangle = \langle b_{\mathbf{m}}^{\dagger} b_{\mathbf{m}} \rangle$ are taken into account in the decoupling, results of Refs. 3,4 are reproduced.

In this paper we try to obtain a better approximation. For this purpose we derive equations of motion for the functions D_3 and D_4 and carry out the decoupling in the many-particle Green's functions which appear in these equations. If in addition to the mentioned correlations we take into account the correlations $\langle a_{\mathbf{l}}^{\dagger} a_{\mathbf{l}+\mathbf{a}_1+\mathbf{a}_2} \rangle$ (where \mathbf{a}_1 and \mathbf{a}_2 are vectors

of nearest neighbors of site zero) and analogous correlations on the second sublattice, we find

$$i\frac{d}{dt}D_3(\mathbf{q}t) = 4\left(C_1 - \frac{1}{2}\right)\delta(t) + \frac{\kappa}{2}\gamma_{\mathbf{q}}D_2(\mathbf{q}t) + \left[\frac{\kappa}{2} + 16C_1\left(C_1 - \frac{1}{2}\right)(1 - \gamma_{\mathbf{q}}^2)\right]D_1(\mathbf{q}t), \quad (7)$$

$$i\frac{d}{dt}D_4(\mathbf{q}t) = 4\left(C_1 - \frac{1}{2}\right)\gamma_{\mathbf{q}}\delta(t) + \frac{\kappa}{2}\gamma_{\mathbf{q}}D_1(\mathbf{q}t) + \left[\frac{\kappa}{2} + 16C_1\left(C_1 - \frac{1}{2}\right)(1 - \gamma_{\mathbf{q}}^2)\right]D_2(\mathbf{q}t),$$

where

$$\kappa = 8\left(\sum_{\mathbf{a}_1}\langle a_{\mathbf{m}+\mathbf{a}_1}^\dagger a_{\mathbf{m}+\mathbf{a}_2}\rangle\langle a_{\mathbf{m}+\mathbf{a}_1} a_{\mathbf{m}+\mathbf{a}_2}^\dagger\rangle - 4C_1^2\right).$$

Owing to the symmetry with respect to translations and rotations the summation in κ does not depend on \mathbf{m} and \mathbf{a}_2 . To derive Eqs. (7) we have taken into account that in accord with the condition of zero site magnetization in the absence of magnetic field in short-range order

$$\langle a_1^\dagger a_1\rangle = \langle b_{\mathbf{m}}^\dagger b_{\mathbf{m}}\rangle = \frac{1}{2}. \quad (8)$$

This condition follows also from constraint (6). Substituting Eqs. (7) into Eqs. (5) we get for the Fourier transforms of Green's functions

$$D_1(\mathbf{q}\omega) = \frac{(4C_1 - \omega)(\omega^2 - \omega_{02}^2) - \frac{\kappa}{2}\left[4\left(C_1 - \frac{1}{2}\right)(1 - \gamma_{\mathbf{q}}^2) - \omega\right]}{(\omega^2 - \omega_1^2)(\omega^2 - \omega_2^2)}, \quad (9)$$

$$D_2(\mathbf{q}\omega) = \frac{4\gamma_{\mathbf{q}}C_1(\omega^2 - \omega_{02}^2) - \frac{\kappa}{2}\omega\gamma_{\mathbf{q}}}{(\omega^2 - \omega_1^2)(\omega^2 - \omega_2^2)},$$

where

$$\omega_{1,2}^2 = \frac{1}{2}(\omega_{01}^2 + \omega_{02}^2 + \kappa) \pm \sqrt{\frac{1}{4}(\omega_{01}^2 - \omega_{02}^2)^2 + \frac{\kappa}{2}(\omega_{01} - \omega_{02})^2 + \frac{\kappa^2}{4}\gamma_{\mathbf{q}}^2}, \quad (10)$$

$$\omega_{01}^2 = 16C_1^2(1 - \gamma_{\mathbf{q}}^2), \quad \omega_{02}^2 = 16\left(C_1 - \frac{1}{2}\right)^2(1 - \gamma_{\mathbf{q}}^2).$$

Green's functions (9) contain two poles ω_1 and ω_2 which correspond to two branches of the magnon spectrum. If κ is set to zero, the second pole disappears in Green's functions and the remaining pole acquires the dispersion of the conventional linear spin-wave theory $\omega_1 = 4C_1(1 - \gamma_{\mathbf{q}}^2)^{1/2}$. For $\kappa \neq 0$ a gap of the width $\kappa^{1/2}$ opens in this branch near $\mathbf{q} = 0$. Simultaneously the second branch acquires finite spectral intensity which is subtracted from the intensity of the first branch. As will be seen below, in the considered temperature range C_1 is close to $\frac{1}{2}$. This allows one to approximate the dispersion of the first branch as $\omega_1 \approx \left[\kappa + 16C_1^2(1 - \gamma_{\mathbf{q}}^2)\right]^{1/2}$ which, with some change of notations, coincides with the dispersion obtained in Refs. 3,4. Technically in those works the gap appears in the magnon spectrum with imposing the constraints of zero staggered or site magnetization, which are incorporated into the Hamiltonian or free energy. In the more exact treatment of the Green's functions the magnon gap arises without such changes of the Hamiltonian.

Parameters C_1 and κ in the above equations contain correlations which can be deduced from Green's functions (9). This gives the following self-consistency conditions for evaluating the parameters:

$$C_1 = \frac{2}{N} \sum_{\mathbf{q}} \gamma_{\mathbf{q}} \mathcal{J}_{\mathbf{q}}, \quad (11)$$

$$\kappa = 8 \left(\frac{3}{4} + 2K_1^2 + K_2^2 - 4C_1^2 \right), \quad (12)$$

where $K_1 = (2/N) \sum_{\mathbf{q}} \mathcal{I}_{\mathbf{q}} \cos(q_x - q_y)$, $K_2 = (2/N) \sum_{\mathbf{q}} \mathcal{I}_{\mathbf{q}} \cos(2q_x)$,

$$\mathcal{J}_{\mathbf{q}} = \frac{4C_1 \gamma_{\mathbf{q}}}{\omega_1^2 - \omega_2^2} \left\{ \frac{\omega_1^2 - \omega_{02}^2}{\omega_1} \left[n(\omega_1) + \frac{1}{2} \right] - \frac{\omega_2^2 - \omega_{02}^2}{\omega_2} \left[n(\omega_2) + \frac{1}{2} \right] \right\}, \quad (13)$$

$$\mathcal{I}_{\mathbf{q}} = \frac{\mathcal{J}_{\mathbf{q}}}{\gamma_{\mathbf{q}}} - \frac{2\kappa \left(C_1 - \frac{1}{2} \right) (1 - \gamma_{\mathbf{q}}^2)}{(\omega_1^2 - \omega_2^2)} \left\{ \frac{1}{\omega_1} \left[n(\omega_1) + \frac{1}{2} \right] - \frac{1}{\omega_2} \left[n(\omega_2) + \frac{1}{2} \right] \right\},$$

$n(\omega) = [\exp(\omega/T) - 1]^{-1}$, q_x and q_y are the components of the wave vector \mathbf{q} (the intersite distance is taken as the unit of length). In Eqs. (11), (12) and below summations over wave vectors are carried out over the magnetic Brillouin zone. Analogously, from Eqs. (9) we find for the spin correlation functions

$$\begin{aligned} \langle \mathbf{S}_l \mathbf{S}_{l'} \rangle &= \left[\frac{2}{N} \sum_{\mathbf{q}} \mathcal{I}_{\mathbf{q}} e^{i\mathbf{q}(l-l')} \right]^2 - \frac{1}{4} \delta_{ll'}, \\ \langle \mathbf{S}_l \mathbf{S}_m \rangle &= - \left[\frac{2}{N} \sum_{\mathbf{q}} \mathcal{J}_{\mathbf{q}} e^{i\mathbf{q}(l-m)} \right]^2. \end{aligned} \quad (14)$$

It can be seen that correlations $\langle S_l^+ S_{l'(m)}^- \rangle$ are zero and only $\langle S_l^z S_{l'(m)}^z \rangle$ contribute in the above expressions. Thus the considered spin-wave approximation is not rotationally invariant.

To determine the parameters C_1 and κ , instead of one of Eqs. (11), (12) one can use the condition of zero site magnetization (8) which can be rewritten as

$$1 = \frac{2}{N} \sum_{\mathbf{q}} \mathcal{I}_{\mathbf{q}}. \quad (15)$$

Comparing results obtained with different pairs of these three equations with Monte Carlo data, we found that the best agreement is achieved with Eqs. (11) and (15). Notice also that all three equations can be used introducing some parameter in addition to κ and C_1 . In particular, such additional parameter appears if we incorporate the constraint of zero staggered magnetization (6) in Hamiltonian (3) with a Lagrange multiplier [condition (15) follows from this constraint, if one takes into account the translation and sublattice symmetry]. This approach is a generalization of the method of Refs. 3,4 — results of these works can be obtained from formulas of the three-parameter approach by setting $\kappa = 0$. We postpone the consideration of this approach to the end of the article. For now we discuss

results obtained in the two-parameter approach based on Eqs. (11) and (15). Notice that the relation $\langle \mathbf{S}_1^2 \rangle = \frac{3}{4}$ follows from Eqs. (14) and (15).

Let us first consider the case of low temperatures. As will be seen below, $\kappa = \mathcal{O}(N^{-2})$ for $T = 0$. Since $q^2 = (2\pi)^2(n_x^2 + n_y^2)/N$ where n_x and n_y are integers, even for the smallest q^2 , excluding $q^2 = 0$, ω_{01}^2 and ω_{02}^2 are much larger than κ for large N . In this case Eqs. (13) can be simplified to

$$\begin{aligned}\mathcal{I}_{\mathbf{q}} &= \frac{4C_1}{\omega_1} \left[n(\omega_1) + \frac{1}{2} \right] + \mathcal{O}(\kappa), \\ \mathcal{J}_{\mathbf{q}} &= \frac{4C_1\gamma_{\mathbf{q}}}{\omega_1} \left[n(\omega_1) + \frac{1}{2} \right] + \mathcal{O}(\kappa).\end{aligned}\tag{16}$$

where $\omega_1 \approx (\omega_{01}^2 + \kappa)^{1/2}$ (here we took into account that $C_1 - \frac{1}{2} \ll C_1$). Notice that the contribution of the gapless magnon mode dropped out from these equations. They are also suitable for an infinite crystal when $T \rightarrow 0$ and κ is exponentially small. With these $\mathcal{I}_{\mathbf{q}}$, $\mathcal{J}_{\mathbf{q}}$ and ω_1 Eqs. (11) and (15) come close to the respective formulas of Ref. 3. As a consequence, in the limit $N \rightarrow \infty$, $T \rightarrow 0$ values of observables obtained with Eqs. (11), (15) are similar to those found in Ref. 3. Therefore we only briefly discuss this limit below.

Using Eqs. (16), for large N and $T = 0$ the sum in the first equation (14) can be written as

$$\frac{2}{N} \sum_{\mathbf{q}} \mathcal{I}_{\mathbf{q}} e^{i\mathbf{q}\mathbf{r}} = \frac{4C_1}{N\sqrt{\kappa}} + \frac{1}{N} \sum_{\mathbf{q} \neq 0} \frac{1}{\sqrt{1 - \gamma_{\mathbf{q}}^2}} e^{i\mathbf{q}\mathbf{r}}.\tag{17}$$

The sublattice magnetization $m_0 = 4C_1/(N\kappa^{1/2})$ is determined by Eq. (15), $m_0 = 1 - N^{-1} \sum_{\mathbf{q} \neq 0} (1 - \gamma_{\mathbf{q}}^2)^{-1/2}$. For an infinite crystal $m_0 = 0.3034$ which is in good agreement with the Monte Carlo calculations.^{9,10} As follows from the above formulas, κ is actually of the order of N^{-2} . From Eq. (17) for large \mathbf{r} we get $m_0 + (2^{1/2}\pi r)^{-1}$ and after analogous transformations in the second equation (14) we find

$$\langle \mathbf{S}_0 \mathbf{S}_{\mathbf{r}} \rangle \approx (-1)^r \left[m_0 + (\sqrt{2}\pi r)^{-1} \right]^2,\tag{18}$$

where $(-1)^r = +1$ or -1 depending on whether the sites $\mathbf{0}$ and \mathbf{r} belong to the same or different sublattices. In Table I the zero-temperature spin correlations $C_{\mathbf{r}} = \langle \mathbf{S}_0 \mathbf{S}_{\mathbf{r}} \rangle$, obtained by numerical solution of Eqs. (11) and (15) (see below), are compared with results of the projected Monte Carlo method.¹⁰ The values agree nicely.

For $N \rightarrow \infty$, $T \rightarrow 0$ we find from Eqs. (11), (15) and (16)

$$\begin{aligned}C_1 &= m_1 - \frac{4}{\pi} \zeta(3) \left(\frac{T}{4m_1} \right)^3 + \mathcal{O}(T^5), \\ \sqrt{\kappa} &= T \exp \left(-\frac{2\pi m_0 m_1}{T} \right) \left[1 + \mathcal{O}(T^2) \right],\end{aligned}\tag{19}$$

where $m_1 = 1 - N^{-1} \sum_{\mathbf{q}} (1 - \gamma_{\mathbf{q}}^2)^{1/2} = 0.57897$ and $\zeta(x)$ is the Riemann zeta function. For large \mathbf{r} the sums in the spin correlations $\langle \mathbf{S}_0 \mathbf{S}_{\mathbf{r}} \rangle$ (14) can be rewritten as

$$\frac{T}{(2\pi)^2 C_1} \iint \frac{d^2 q}{q^2 + (2\xi)^{-2}} e^{i\mathbf{q}\mathbf{r}} \approx \frac{T}{2C_1} \sqrt{\frac{\xi}{\pi r}} \exp \left(-\frac{r}{2\xi} \right)$$

with the correlation length

$$\xi = C_1 \sqrt{\frac{2}{\kappa}} = \frac{\sqrt{2}m_1}{T} \exp\left(\frac{2\pi m_0 m_1}{T}\right) [1 + \mathcal{O}(T^2)]. \quad (20)$$

This value of the correlation length is in agreement with results obtained in Refs. 1,2.

To solve Eqs. (11) and (15) for arbitrary T and N we determined the minimum of the function

$$F(C_1, \kappa) = \left(1 - \frac{2}{N} \sum_{\mathbf{q}} \mathcal{I}_{\mathbf{q}}\right)^2 + \left(1 - \frac{2}{NC_1} \sum_{\mathbf{q}} \gamma_{\mathbf{q}} \mathcal{J}_{\mathbf{q}}\right)^2,$$

which is constructed from squares of the differences of the right and left sides of these equations. The iteration procedure with the steepest descent method was continued until F was less than 10^{-12} . As an example, parameters obtained by this procedure for a 20×20 lattice are given in Table II. These parameters were used for calculating the static uniform susceptibility

$$\begin{aligned} \chi &= \frac{1}{T} \sum_{\mathbf{r}} \langle S_0^z S_{\mathbf{r}}^z \rangle = \frac{1}{3T} \sum_{\mathbf{r}} \langle \mathbf{S}_0 \mathbf{S}_{\mathbf{r}} \rangle \\ &= \frac{1}{3T} \left[\frac{2}{N} \sum_{\mathbf{q}} (\mathcal{I}_{\mathbf{q}}^2 - \mathcal{J}_{\mathbf{q}}^2) - \frac{1}{4} \right] \end{aligned} \quad (21)$$

and the energy per spin

$$E = 2 \langle \mathbf{S}_1 \mathbf{S}_{1+\mathbf{a}} \rangle = -2C_1^2. \quad (22)$$

Results for a 20×20 lattice are shown in Figs. 1 and 2 together with the data obtained in the Monte Carlo calculations^{11,12} and in the modified spin-wave theory of Refs. 3,4. As seen from the figures, results obtained in the spin-wave approximations of the present work and of Refs. 3,4 are close and are in good agreement with the Monte Carlo results in the considered temperature range. The size dependence of χ and E calculated with the above formulas is negligible for large enough lattices — the difference between values obtained for a 40×40 lattice and those shown in Figs. 1 and 2 is less than the size of symbols in these figures. Notice also that zero frequency of the second branch at $\mathbf{q} = 0$ does not lead to divergencies in the above formulas as the respective numerators in Eqs. (13) approach zero sufficiently rapidly when $\mathbf{q} \rightarrow 0$.

As seen from Table II, starting from low temperatures the gap determined by κ grows with T . With this growth the spectral intensity of the second branch and its contribution to the observables increases. However, near $T = 0.5$ κ starts to decrease. For $T \approx 0.7$, when $\kappa \rightarrow 0$ and $C_1 \approx 0.5$, the considered two-parameter approximation ceases to work — it is impossible to find parameters for which Eqs. (11) and (15) are fulfilled with high accuracy.

Now let us consider the three-parameter approximation mentioned above. The additional parameter is the Lagrange multiplier λ with which the terms $\sum_{\mathbf{l}} a_{\mathbf{l}}^\dagger a_{\mathbf{l}} + \sum_{\mathbf{m}} b_{\mathbf{m}}^\dagger b_{\mathbf{m}}$ are added to Hamiltonian (3) to ensure the fulfillment of constraint (6). With these additional terms $D_1(\mathbf{q}\omega)$ in Eq. (9), κ in Eq. (12) and $\mathcal{I}_{\mathbf{q}}$ in Eq. (13) are slightly changed

$$D_1(\mathbf{q}\omega) = \frac{(4C_1\eta^{-1} - \omega)(\omega^2 - \omega_{02}^2) - \frac{\kappa}{2} \left[4 \left(C_1 - \frac{1}{2} \right) (1 - \gamma_{\mathbf{q}}^2) - \omega \right]}{(\omega^2 - \omega_1^2)(\omega^2 - \omega_2^2)}, \quad (9')$$

$$\kappa = 8 \left[\frac{3}{4} + 2K_1^2 + K_2^2 + 4C_1^2 \left(1 - \frac{2}{\eta} \right) \right], \quad (12')$$

$$\mathcal{I}_{\mathbf{q}} = \frac{\mathcal{J}_{\mathbf{q}}}{\eta\gamma_{\mathbf{q}}} - \frac{2\kappa \left(C_1 - \frac{1}{2} \right) (1 - \gamma_{\mathbf{q}}^2)}{(\omega_1^2 - \omega_2^2)} \left\{ \frac{1}{\omega_1} \left[n(\omega_1) + \frac{1}{2} \right] - \frac{1}{\omega_2} \left[n(\omega_2) + \frac{1}{2} \right] \right\}, \quad (13')$$

whereas $D_2(\mathbf{q}\omega)$ in Eq. (9), $\mathcal{J}_{\mathbf{q}}$ in Eq. (13), Eqs. (11), (15), (21) and (22) retain their form. In these equations $\eta = [1 - \lambda/(4C_1)]^{-1}$,

$$\begin{aligned} \omega_{1,2}^2 &= \frac{1}{2} (\omega_{01}^2 + \omega_{02}^2 + \kappa) \\ &\pm \sqrt{\frac{1}{4} (\omega_{01}^2 - \omega_{02}^2)^2 + \frac{\kappa}{2} (\omega_{01}^2 + \omega_{02}^2) - 16C_1 \left(C_1 - \frac{1}{2} \right) \frac{\kappa}{\eta} (1 - \gamma_{\mathbf{q}}^2) + \frac{\kappa^2}{4} \gamma_{\mathbf{q}}^2}, \quad (10') \\ \omega_{01}^2 &= 16C_1^2 \left(\frac{1}{\eta^2} - \gamma_{\mathbf{q}}^2 \right), \quad \omega_{02}^2 = 16 \left(C_1 - \frac{1}{2} \right)^2 (1 - \gamma_{\mathbf{q}}^2). \end{aligned}$$

To solve Eqs. (11), (12') and (15) we determined the minimum of the function $F'(C_1, \kappa, \eta)$, constructed from squares of the differences of left and right sides of these equations, by the steepest descent method. The static uniform susceptibility and the energy per spin calculated with the parameters obtained in this way for a 20×20 lattice are shown in Figs. 1 and 2. As seen from the figures, in comparison with the two-parameter approximation the three-parameter approach agrees slightly better with the Monte Carlo results and is applicable in the wider temperature range $0 \leq T \lesssim 0.8$. However, the convergence of the steepest descent method in the three-parameter approximation is much worse than in the two-parameter one. We connect this with the observation that both approaches give similar pictures of magnon modes and in the three-parameter approximation the two parameters κ and λ (or η) determine one physical quantity — the magnon gap. In this approximation the worsened convergence is connected with the flat minimum of F' considered as the function of κ and λ .

In the present work we have found the gapless mode in the state with short-range order. In ordered states excitations of such type correspond to Goldstone's mode and point to the existence of the continuous degeneracy of these states.¹³ The observation of the gapless mode in the considered disordered state may also be connected with the continuous degeneracy of this state. In some respects a similar magnon spectrum of short-range order was obtained in Refs. 14,15. When considered in the magnetic Brillouin zone the spectrum consists also of two modes one of which has a gap near $\mathbf{q} = 0$ and another is gapless. However, the shape of these branches, their relative spectral intensities and temperature behavior differ essentially from those obtained here. The spin-wave approximations of Refs. 14,15 are rotationally invariant but are not self-consistent — correction coefficients and data of other calculations are needed to fit results to experiment in the temperature range $T \lesssim 1$.

In conclusion, the spin-wave theory of short-range order in the square lattice Heisenberg antiferromagnet was formulated. In agreement with previously obtained results we found that as soon as the temperature exceeds zero and long-range order gives way to short-range order a gap opens in the conventional magnon mode near $\mathbf{q} = 0$. We found additionally that a new gapless mode arises simultaneously with opening the gap. With growing temperature the spectral intensity is redistributed from the conventional to the gapless mode.

We considered spin-wave approximations with two and three self-consistently determined parameters. For low temperatures and large crystals the theory reproduces results of the modified spin-wave theory of Refs. 3,4. Without fitting parameters our calculations give values of the static uniform susceptibility and energy per spin in good agreement with Monte Carlo results in the temperature range $0 \leq T \lesssim 0.8J$ where J is the exchange constant.

ACKNOWLEDGMENTS

This work was partially supported by the ESF grant No. 2688 and by the WTZ grant (Project EST-003-98) of the BMBF.

REFERENCES

- ¹ D. A. Arovas and A. Auerbach, Phys. Rev. B **38**, 316 (1988).
- ² S. Chakravarty, B. I. Halperin, and D. R. Nelson, Phys. Rev. B **39**, 2344 (1989).
- ³ M. Takahashi, Phys. Rev. B **40**, 2494 (1989).
- ⁴ S. Tang, M. E. Lazzouni, and J. E. Hirsch, Phys. Rev. B **40**, 5000 (1989).
- ⁵ A. V. Chubukov, S. Sachdev, and J. Ye, Phys. Rev. B **49**, 11919 (1994).
- ⁶ N. D. Mermin and H. Wagner, Phys. Rev. Lett. **17**, 1133 (1966).
- ⁷ A. Sherman and M. Schreiber, Physica C **303**, 246 (1998).
- ⁸ S. V. Tyablikov, *Methods of the Quantum Theory of Magnetism* (Plenum Press, New York, 1967).
- ⁹ J. D. Reger and A. P. Young, Phys. Rev. B **37**, 5978 (1988).
- ¹⁰ S. Liang, Phys. Rev. B **42**, 6555 (1990).
- ¹¹ Y. Okabe and M. Kikuchi, J. Phys. Soc. Japan **57**, 4351 (1988).
- ¹² M. S. Makivić and H.-Q. Ding, Phys. Rev. B **43**, 3562 (1991).
- ¹³ D. Forster, *Hydrodynamic Fluctuations, Broken Symmetry and Correlation Functions* (W. A. Benjamin, Inc., London, 1975).
- ¹⁴ H. Shimahara and S. Takada, J. Phys. Soc. Japan **60**, 2394 (1991).
- ¹⁵ A. Sokol, R. R. P. Singh, and N. Elstner, Phys. Rev. Lett. **76**, 4416 (1996).

FIGURES

FIG. 1. The static uniform susceptibility obtained in the Monte Carlo simulation for a 12×12 lattice¹¹ (\bullet), in the modified spin-wave approximation of Refs. 3,4 (\circ) and in the two-parameter ($+$) and three-parameter (\times) spin-wave approximations of the present work. In the spin-wave calculations a 20×20 lattice was used.

FIG. 2. The energy per spin obtained in the Monte Carlo simulation¹² (\bullet), in the modified spin-wave approximations of Refs. 3,4 (\circ) and in the two-parameter ($+$) and three-parameter (\times) spin-wave approximations of the present work. In the spin-wave calculations a 20×20 lattice was used.

TABLES

TABLE I. The zero-temperature spin correlations $C_{\mathbf{r}}$ obtained with the two-parameter spin-wave approximation (SW) for a 20×20 lattice in comparison with the projected Monte Carlo data (PMC).¹⁰

	PMC	SW
$C_{1,0}$	-0.3348	-0.3354
$C_{1,1}$	0.2028	0.2016
$C_{2,0}$	0.1772	0.1751
$C_{2,1}$	-0.1671	-0.1648
$C_{2,2}$	0.1475	0.1454
$C_{3,0}$	-0.1491	-0.1461
$C_{3,1}$	0.1430	0.1404

TABLE II. Parameters C_1 and κ obtained from Eqs. (11) and (15) for a 20×20 lattice.

T	C_1	κ
10^{-5}	0.57912	$2.773 \cdot 10^{-4}$
0.1	0.57904	$4.685 \cdot 10^{-4}$
0.2	0.57826	$9.390 \cdot 10^{-4}$
0.3	0.57543	$1.443 \cdot 10^{-3}$
0.4	0.56819	$1.941 \cdot 10^{-3}$
0.5	0.55409	$2.303 \cdot 10^{-3}$
0.6	0.53037	$2.093 \cdot 10^{-3}$
0.7	0.50003	$3.664 \cdot 10^{-6}$

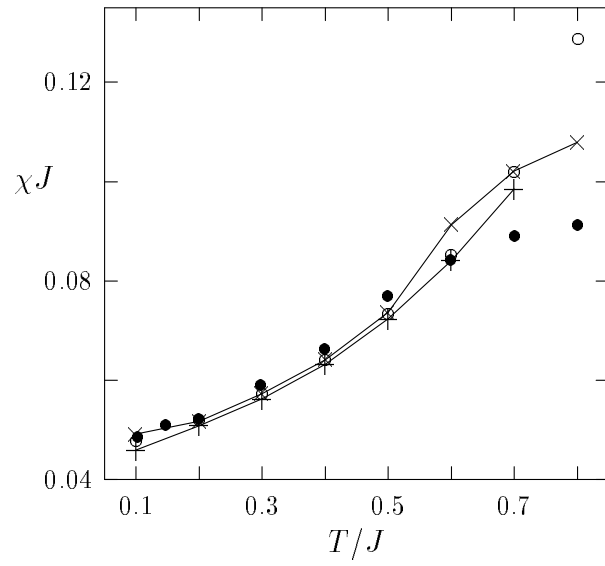


Fig. 1. A. Sherman and M. Schreiber, Temperature behavior . . .

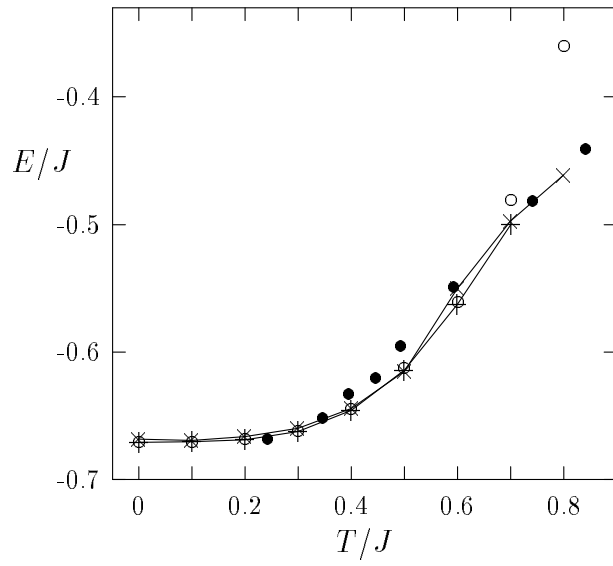


Fig. 2. A. Sherman and M. Schreiber, Temperature behavior ...